

**$^{15}\text{C}$ - $^{15}\text{F}$  Charge Symmetry and the  $^{14}\text{C}(n, \gamma)^{15}\text{C}$  Reaction Puzzle**N. K. Timofeyuk,<sup>1</sup> D. Baye,<sup>2</sup> P. Descouvemont,<sup>2</sup> R. Kamouni,<sup>2</sup> and I. J. Thompson<sup>1</sup><sup>1</sup>*Department of Physics, University of Surrey, Guildford, Surrey GU2 7XH, United Kingdom*<sup>2</sup>*PNTPM CP229, Université Libre de Bruxelles, B1050 Brussels, Belgium*

(Received 8 November 2005; published 27 April 2006)

The low-energy reaction  $^{14}\text{C}(n, \gamma)^{15}\text{C}$  provides a rare opportunity to test indirect methods for the determination of neutron capture cross sections by radioactive isotopes versus direct measurements. It is also important for various astrophysical scenarios. Currently, puzzling disagreements exist between the  $^{14}\text{C}(n, \gamma)^{15}\text{C}$  cross sections measured directly, determined indirectly, and calculated theoretically. To solve this puzzle, we offer a strong test based on a novel idea that the amplitudes for the virtual  $^{15}\text{C} \rightarrow ^{14}\text{C} + n$  and the real  $^{15}\text{F} \rightarrow ^{14}\text{O} + p$  decays are related. Our study of this relation, performed in a microscopic model, shows that existing direct and some indirect measurements strongly contradict charge symmetry in the  $^{15}\text{C}$  and  $^{15}\text{F}$  mirror pair. This brings into question the experimental determinations of the astrophysically important  $(n, \gamma)$  cross sections for short-lived radioactive targets.

DOI: 10.1103/PhysRevLett.96.162501

PACS numbers: 25.40.Lw, 21.60.Gx, 27.20.+n

Many nuclear reactions in stellar interiors involve radioactive nuclei. Construction of radioactive beam facilities all around the world provided the opportunity to study some of these reactions directly. However, a large class of nuclear reactions, namely, neutron capture by short-lived radioactive isotopes, cannot be studied directly due to the nonexistence of neutron targets and the short neutron lifetime. Nevertheless, since the knowledge of these reactions is important for predictions of chemical evolution of the Universe they are studied indirectly, for example, using inverse dissociation reactions, and will be done so for a long time in the future. Therefore, the consistency between direct and indirect methods must be achieved.

The neutron capture on a long-lived radioactive target  $^{14}\text{C}$  provides one of the few possible test cases where a comparison between direct and indirect methods is possible. On the other hand, the  $^{14}\text{C}(n, \gamma)^{15}\text{C}$  reaction is interesting on its own because of its important astrophysical applications. First, the knowledge of this reaction rate is necessary for making quantitative predictions for primordial abundances of heavy chemical elements in a non-standard inhomogeneous big bang model. According to this model, neutron- and proton-rich zones may appear in the early Universe with different sequences of nuclear reactions in them. In neutron-rich zones, reaction chains composed of  $(n, \gamma)$ ,  $(t, n)$ , and  $(\alpha, n)$  reactions allow bypassing of the  $A = 8$  mass gap and the production of beryllium, boron, and carbon isotopes including stable ones on the time scale of the big bang isotope  $^{14}\text{C}$  [1]. Further nucleosynthesis depends on reactions that destroy  $^{14}\text{C}$ , the most important of which is  $^{14}\text{C}(n, \gamma)^{15}\text{C}$ . Second,  $^{14}\text{C}(n, \gamma)^{15}\text{C}$  is a part of the neutron induced CNO cycles in the helium burning layer of asymptotic giant branch stars, in the core helium burning of massive stars, and in subsequent carbon burning [2]. Such cycles may cause a depletion in the CNO abundances. The  $^{14}\text{C}(n, \gamma)^{15}\text{C}$  reaction is the slowest of both of these cycles and, therefore the knowledge of its rate is important to predict the  $^{14}\text{C}$  abun-

dances over the period of high neutron flux [2]. Finally, the  $^{14}\text{C}(n, \gamma)^{15}\text{C}$  reaction triggers synthesis of heavy carbon and oxygen isotopes in the hot-bubble scenario of gravitational core-collapse Type II supernovae explosions with neutrino driven winds [3].

Currently, a puzzling disagreement exists between the cross sections  $\sigma_{n,\gamma}$  of  $^{14}\text{C}(n, \gamma)^{15}\text{C}$  measured directly, determined indirectly, and calculated theoretically. The first direct measurements in Ref. [4] provided  $\sigma_{n,\gamma} = 1.1 \pm 0.28 \mu\text{b}$  which is about 5 times smaller than the theoretical value of  $5.1 \mu\text{b}$  predicted earlier in Ref. [5] within a potential model. The subsequent folding model calculations [6] and microscopic cluster model calculations [7] have confirmed the large value of Ref. [5]. Recently, the  $^{14}\text{C}(n, \gamma)^{15}\text{C}$  cross sections have been determined indirectly in three dissociation experiments of  $^{15}\text{C}$  [8–10]. In these works,  $\sigma_{n,\gamma}(23.3 \text{ keV})$  has been obtained from the fit to the data at higher energies providing  $2.6 \pm 0.9 \mu\text{b}$  [8],  $4.4 \pm 0.6 \mu\text{b}$  [9], and  $4.1 \pm 0.4 \mu\text{b}$  [10]. Last year, new direct measurements of  $\sigma_{n,\gamma}$  have been reported in Ref. [11]. They suggest that  $\sigma_{n,\gamma}(23.3 \text{ keV}) = 2.7 \pm 0.2 \mu\text{b}$ , which is twice the value from the first direct measurements.

In this Letter, we propose to use charge symmetry between  $^{15}\text{C}(\frac{1}{2}^+)$  and its isobar analog  $^{15}\text{F}(\frac{1}{2}^+)$  as a strong and model-independent tool to discriminate between different determinations and predictions for the  $^{14}\text{C}(n, \gamma)^{15}\text{C}$  cross sections.

Let us notice first that the main contribution to the  $^{14}\text{C}(n, \gamma)^{15}\text{C}$  reaction rate comes from the direct  $E1$  capture from the initial  $p$  wave to the relatively weakly bound  $\frac{1}{2}^+$  ground state of  $^{15}\text{C}$ . This capture occurs well outside the  $^{14}\text{C}$  interior, which we demonstrate in Fig. 1 by plotting the integrand of the  $E1$  amplitude  $M_{n,\gamma}^{(E1)}$  for the  $(n, \gamma)$  reaction

$$M_{n,\gamma}^{(E1)} \sim \int_0^\infty dr r^3 \varphi_{\text{sc}}(r) I(r) \quad (1)$$

as a function of the distance  $r$  between  $n$  and  $^{14}\text{C}$ . In

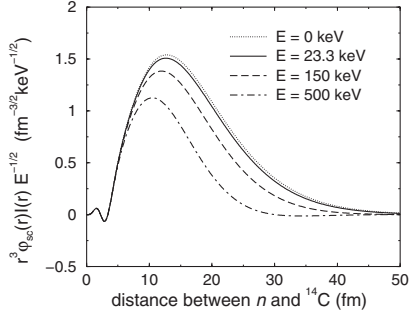


FIG. 1. Integrand for the  $E1$  amplitude of the  $^{14}\text{C}(n, \gamma)^{15}\text{C}$  reaction times  $E^{-1/2}$  for various incident neutron energies  $E$ .  $\varphi_{\text{sc}}(r)$  and  $I(r)$  have been calculated using the potential model parameters from Ref. [5].

Eq. (1),  $\varphi_{\text{sc}}(r)$  is the neutron scattering wave function in the entrance channel and  $I(r)$  is the radial part of the overlap integral  $\langle ^{14}\text{C}|^{15}\text{C}\rangle$ . In this case,  $M_{n,\gamma}^{(E1)}$  is mostly determined by the  $I(r)$  tail that behaves as

$$\sqrt{15}I(r) \approx C_n e^{-\kappa_n r}/r, \quad r \rightarrow \infty. \quad (2)$$

Here  $C_n$  is the neutron asymptotic normalization coefficient (ANC),  $\kappa_n = \sqrt{2\mu\epsilon_n}/\hbar$ ,  $\epsilon_n$  is the neutron separation energy in  $^{15}\text{C}$  and  $\mu$  is the  $n + ^{14}\text{C}$  reduced mass. The factor  $\sqrt{15}$  accounts for antisymmetrization. The  $(n, \gamma)$  cross sections are therefore determined by the ANC squared  $C_n^2$  and all theoretical models using the same  $C_n^2$  should provide approximately the same  $\sigma_{n,\gamma}$ .

In this Letter, we determine  $C_n^2$  using a recently established relation between the neutron ANC of a bound state and the proton width  $\Gamma_p$  of its mirror analog resonance [12], which follows from the charge symmetry of one-nucleon decay amplitudes. As shown in Ref. [12], the ratio

$$\mathcal{R}_\Gamma = \Gamma_p/C_n^2, \quad (3)$$

for narrow resonances can be approximated by a model-independent analytical expression that contains the neutron separation energy, the energy  $E_R$  of the proton resonance, charge of the core, and the range of the strong interaction between the last neutron (or proton) and the core. However, this expression may not be accurate for the broad  $s$ -wave resonance  $^{15}\text{F}(\frac{1}{2}^+)$ . To predict  $\mathcal{R}_\Gamma$  more reliably in this case, more accurate model calculations should be performed. The only requirement for a model should be its ability to reproduce exactly the asymptotic behavior of the valence neutron in  $^{15}\text{C}$  given by Eq. (2) and its applicability to the elastic scattering calculations. The microscopic cluster model (MCM) of the type we used in [13] is well suited for such calculations. Previous study of some broad  $s$ -wave resonances within this model has shown that  $\mathcal{R}_\Gamma$  is not very sensitive to model assumptions even if  $C_n^2$  and  $\Gamma_p$  strongly depend on them [13]. The theoretical uncertainty of  $\mathcal{R}_\Gamma$  is less than 10% [13]. A similar uncertainty in  $\mathcal{R}_\Gamma$  for the  $^{15}\text{C}$ - $^{15}\text{F}$  mirror pair would be sufficient to determine

$C_n^2$  and, therefore, to predict  $\sigma_{n,\gamma}$  accurately enough to reduce its uncertainty from the current factor of 5.

To calculate  $\mathcal{R}_\Gamma$ , we use the MCM from Ref. [14] where  $^{15}\text{C}$  ( $^{15}\text{F}$ ) is represented by the  $^{14}\text{C} + n$  ( $^{14}\text{O} + p$ ) configuration. The internal structure of  $^{14}\text{C}$  ( $^{14}\text{O}$ ) is described by the  $0p$  translation-invariant oscillator shell model. We performed both single-channel and multichannel calculations. In the latter case, we have taken into account the  $0_2^+$ ,  $1^+$ , and  $2_{1,2}^+$  core excitations. Each calculation has been performed with two values of the oscillator radius, 1.5 fm and 1.75 fm. We use effective nucleon-nucleon (NN) interactions well adapted for such calculations, the Volkov potential V2 [15] and the Minnesota (MN) potential [16]. The two-body spin-orbit force [17] with  $S_0 = 30 \text{ MeV fm}^5$  and the Coulomb interaction are also included. Both V2 and MN have one adjustable parameter that gives the strength of the odd NN potentials  $V_{11}$  and  $V_{33}$ . We fit this parameter in each case to reproduce the experimental values for  $\epsilon_n$  or  $E_R$ . Slightly different adjustable parameters in  $^{15}\text{C}$  and  $^{15}\text{F}$ , needed to reproduce  $\epsilon_n$  and  $E_R$ , simulate charge symmetry breaking of the effective NN interactions.

First, we calculate  $\mathcal{R}_\Gamma$  assuming for  $E_R$  the value of 1.47 MeV obtained in Ref. [14] using an  $R$ -matrix analysis of the  $^{14}\text{O} + p$  scattering measured in Ref. [18]. The resulting value of  $\mathcal{R}_\Gamma$  changes from 0.280 to 0.313 MeV · fm with different model assumptions and NN potentials (see Table I). We adopt its average value  $\mathcal{R}_\Gamma = 0.297 \pm 0.017 \text{ MeV} \cdot \text{fm}$ . Using the experimental value  $\Gamma_p = 0.56 \text{ MeV}$  from Ref. [14], we obtain from Eq. (3) for  $^{15}\text{C}$  the  $C_n^2$  value equal to  $1.89 \pm 0.11 \text{ fm}^{-1}$ . Below, we refer to  $C_n^2$  obtained using  $\mathcal{R}_\Gamma$  from the MCM calculations as  $C_{\text{mir}}^2$ .

Often, a two-body potential model is used to predict the  $\langle ^{14}\text{C}|^{15}\text{C}\rangle$  overlap. For the magnitude of its tail to be determined by  $C_{\text{mir}}$ , the single-particle wave function should be multiplied by a spectroscopic amplitude  $S_{\text{mir}}^{1/2} = C_{\text{mir}}/b_{\text{s.p.}}$ , where  $b_{\text{s.p.}}$  is the single-particle ANC obtained in such a model. Table II shows  $S_{\text{mir}}$  for a range of the Woods-Saxon potentials used in earlier work.  $S_{\text{mir}}$  from the first four lines agrees with the spectroscopic factors either determined or used in these works,  $S_{\text{exp}}$ , within the error bars. The corresponding ANCs squared  $C_{\text{exp}}^2 = S_{\text{exp}} b_{\text{s.p.}}^2$  also agree with  $C_{\text{mir}}^2$  within the error bars. These  $C_{\text{exp}}^2$  were used in the analysis of the  $^{14}\text{C}(d, p)^{15}\text{C}$  reaction within the distorted wave Born approximation [19], direct  $(n, \gamma)$  calculations [5], time-dependent [20], and distorted

TABLE I. Ratio  $\mathcal{R}_\Gamma$  (in MeV · fm) calculated in the single-channel and multichannel MCM with two different oscillator radii  $b$  and two different NN potentials.

	single-channel MCM		multichannel MCM	
	$b = 1.5 \text{ fm}$	$b = 1.75 \text{ fm}$	$b = 1.5 \text{ fm}$	$b = 1.75 \text{ fm}$
V2	0.297	0.280	0.301	0.286
MN	0.309	0.291	0.313	0.297

TABLE II. The depth  $V_0$  (in MeV), radius  $r_0$  and diffuseness  $a$  (in fm) of the Woods-Saxon potentials, the single-particle ANC  $b_{s.p.}$  (in  $\text{fm}^{-1/2}$ ), the spectroscopic factor  $S_{\text{exp}}$  for the works listed in the first column and the corresponding ANC squared  $C_{\text{exp}}^2 = S_{\text{exp}} b_{s.p.}^2$  (in  $\text{fm}^{-1/2}$ ). Also shown are the spectroscopic factor  $S_{\text{mir}} = (C_{\text{mir}}/b_{s.p.})^2$ , corresponding to  $C_{\text{mir}}^2 = 1.89 \pm 0.11 \text{ fm}^{-1}$ , the coefficients  $S(0)$  (in  $10^{20} \text{ fm}^3 \text{ s}^{-1}$ ),  $s_1$  (in  $\text{MeV}^{-1}$ ) and  $s_2$  (in  $\text{MeV}^{-2}$ ) in the Taylor expansion of  $\sigma_{n,\gamma}$  [Eq. (4)] and the  $\sigma_{n,\gamma}$  value at 23.3 keV (in  $\mu\text{b}$ ), calculated with the corresponding values of  $V_0$ ,  $r_0$ ,  $a$ , and  $S_{\text{mir}}$ .

Ref.	$V_0$	$r_0$	$a$	$b_{s.p.}$	$S_{\text{exp}}$	$C_{\text{exp}}^2$	$S_{\text{mir}}$	$S(0)$	$s_1$	$s_2$	$\sigma_{n,\gamma}(23.3 \text{ keV})$
[5]	48.65	1.261	0.7	1.48	0.88	1.92	$0.87 \pm 0.05$	$11.4 \pm 0.65$	-0.843	0.540	$5.35 \pm 0.30$
[19]	46.46	1.3	0.7	1.49	0.88	1.96	$0.85 \pm 0.05$	$11.3 \pm 0.65$	-0.846	0.541	$5.33 \pm 0.30$
[20]	52.79	1.228	0.6	1.38	1.0	1.91	$0.99 \pm 0.06$	$11.3 \pm 0.65$	-0.872	0.607	$5.32 \pm 0.30$
[21]	49.29	1.25	0.7	1.47	$0.97 \pm 0.08$	$2.10 \pm 0.15$	$0.87 \pm 0.07$	$11.3 \pm 0.65$	-0.842	0.539	$5.32 \pm 0.30$
[21]	44.29	1.25	0.7	1.47	$0.73 \pm 0.05$	$1.58 \pm 0.11$	$0.87 \pm 0.07$	$11.3 \pm 0.65$	-0.842	0.539	$5.32 \pm 0.30$
[21]	61.17	1.15	0.5	1.28	$0.92 \pm 0.07$	$1.50 \pm 0.08$	$1.16 \pm 0.06$	$11.3 \pm 0.65$	-0.882	0.637	$5.32 \pm 0.30$
[22]	55.36	1.223	0.5	1.30	0.90	1.53	$1.11 \pm 0.07$	$11.2 \pm 0.65$	-0.894	0.652	$5.28 \pm 0.30$
[18]	54.15	1.17	0.71	1.45			$0.90 \pm 0.05$	$11.4 \pm 0.65$	-0.834	0.530	$5.36 \pm 0.30$

wave [21] analysis of the  $^{15}\text{C}$  breakup. The  $C_{\text{exp}}^2$  and  $S_{\text{exp}}$  values from the next three lines, obtained in the plane-wave analysis of the Coulomb breakup [21] and from knockout [22], are smaller than  $C_{\text{mir}}^2$  and  $S_{\text{mir}}$  by  $\sim 25\%$ .

This discrepancy may originate due to either insufficient understanding of one-nucleon removal reactions, or to underestimating the  $\mathcal{R}_\Gamma$ . According to Ref. [13],  $\mathcal{R}_\Gamma$  can have large uncertainties either in components with small spectroscopic factors, or in the presence of strong core excitations. In  $^{15}\text{C}$ , the core excitations are not significant and the  $^{14}\text{C}_{\text{g.s.}} + n$  configuration dominates. Thus, there is no room for increasing  $\mathcal{R}_\Gamma$  by 25% unless we have fitted the theoretical position of the resonance at a wrong energy. To verify this, we repeat the MCM calculations using different values of  $E_R$  and  $\Gamma_p$  from the literature, as given in Table III. The predicted  $\mathcal{R}_\Gamma$  and  $C_{\text{mir}}^2$  are shown in Table III. In general, the new  $C_{\text{mir}}^2$  are larger than the one obtained with  $E_R = 1.47 \text{ MeV}$  and  $\Gamma_p = 0.56 \text{ MeV}$ . They may agree with  $C_{\text{exp}}^2$  derived from the plane-wave analysis of the Coulomb breakup [21] and from neutron knockout [22] only if the largest values of  $E_R$  combined with the lowest  $\Gamma_p$  values from the intervals given in Refs. [24,26] are assumed.

Large  $C_{\text{mir}}^2$ , obtained for  $E_R$  and  $\Gamma_p$  from Refs. [18,23–27], give large spectroscopic factors  $S_{\text{mir}} = (C_{\text{mir}}/b_{s.p.})^2$

(see Table III), which in most cases are larger than the prediction of  $(15/14)^2 \approx 1.15$  from the simplest version of the translation-invariant shell model. This value follows from the Pauli principle applied to 15 nucleons occupying the lowest shell model states. Any other occupancy of energy levels decreases the spectroscopic factor. Therefore, the inequality  $S_{\text{mir}} \leq 1.15$  can serve as a tool for identifying physically meaningful values of  $E_R$  and  $\Gamma_p$ . From this point of view,  $E_R$  and  $\Gamma_p$  from Ref. [25] can be discarded. The same concerns the values  $E_R = 1.29 \text{ MeV}$  and  $\Gamma_p = 0.7 \text{ MeV}$  from Ref. [18]. However, other intervals for  $E_R$  and  $\Gamma_p$  from Table III can be narrowed down to satisfy the  $S_{\text{mir}} \leq 1.15$  condition. The values  $E_R = 1.47 \text{ MeV}$  and  $\Gamma_p = 0.56 \text{ MeV}$  give the most reasonable range for  $S_{\text{mir}}$ . Therefore, we use the  $C_{\text{mir}}^2 = 1.89 \pm 0.11 \text{ fm}^{-1}$  value obtained with them to predict the  $^{14}\text{C}(n, \gamma)^{15}\text{C}$  cross sections.

To calculate  $\sigma_{n,\gamma}$ , we use the new representation of the low-energy  $(n, \gamma)$  cross sections introduced in Ref. [28]. For  $E1$  capture from a  $p$  wave it reads

$$\sigma_{n,\gamma}(E) \approx \frac{\mu\sqrt{2\mu E}}{\hbar^2} S(0)(1 + s_1 E + s_2 E^2). \quad (4)$$

In Eq. (4) the coefficient  $S(0)$  is the analog of the astro-

TABLE III. The energy  $E_R$  and the width  $\Gamma_p$  of the  $^{15}\text{F}(\frac{1}{2}^+)$  resonance (in MeV) from the references in the first column, the MCM value of  $\mathcal{R}_\Gamma$  corresponding to  $E_R$ , the neutron ANC squared  $C_{\text{mir}}^2$  in  $^{15}\text{C}$  (in  $\text{fm}^{-1/2}$ ) and the spectroscopic factor  $S_{\text{mir}} = (C_{\text{mir}}/b_{s.p.})^2$  compatible with this ANC.  $S_{\text{mir}}$  has been calculated using all the  $b_{s.p.}$  values from Table II.

Ref.	$E_R$	$\Gamma_p$	$\mathcal{R}_\Gamma$	$C_{\text{mir}}^2$	$S_{\text{mir}}$
[23]	$1.6 \pm 0.2$	$\geq 0.9$	$0.352 \pm 0.111$	$\geq 1.94$	$\geq 0.87$
[24]	$1.37 \pm 0.18$	$0.8 \pm 0.3$	$0.250 \pm 0.089$	$3.20_{-1.73}^{+3.59}$	$2.41 \pm 1.75$
[25]	$1.51 \pm 0.11$	1.2	$0.307 \pm 0.067$	$4.10 \pm 0.88$	$2.25 \pm 0.81$
[26]	$1.41 \pm 0.15$	$0.8 \pm 0.3$	$0.260 \pm 0.073$	$3.08_{-1.57}^{+2.83}$	$2.15 \pm 1.48$
[18]	$1.45_{-0.10}^{+0.16}$	0.7	$0.295 \pm 0.073$	$2.37_{-0.47}^{+0.78}$	$1.39 \pm 0.54$
[18]	$1.29_{-0.06}^{+0.08}$	0.7	$0.212 \pm 0.036$	$3.30_{-0.48}^{+0.70}$	$1.86 \pm 0.60$
[14]	1.47	0.56	$0.297 \pm 0.017$	$1.89 \pm 0.11$	$1.01 \pm 0.21$
[27]	$1.23 \pm 0.05$	$0.67 \pm 0.17$	$0.194 \pm 0.029$	$3.45_{-1.22}^{+1.64}$	$2.06 \pm 1.06$

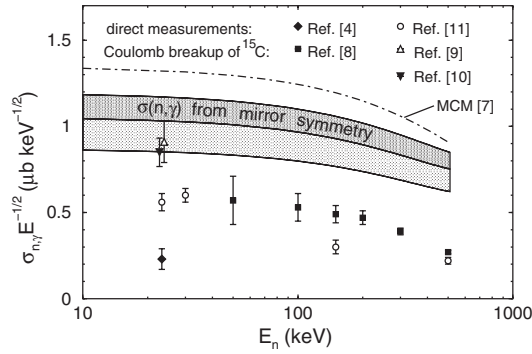


FIG. 2. Experimental (data points) and theoretical values of  $\sigma_{n,\gamma}E^{-1/2}$ . The dark shadowed area corresponds to  $\sigma_{n,\gamma}$  derived from mirror symmetry assuming  $E_R$  and  $\Gamma_p$  from Ref. [14] while the light one corresponds to all other  $E_R$  and  $\Gamma_p$  consistent with  $S_{\text{mir}} \leq 1.15$ . The dot-dashed curve represents the MCM calculations from [7].

physical  $S$  factor for neutrons and is given by an integral (1) that contains the zero energy limit of  $\varphi_{\text{sc}}(r)$ . Two other coefficients,  $s_1$  and  $s_2$ , contain first and second energy derivatives of  $\varphi_{\text{sc}}(r)$  at  $E = 0$ . The latter is calculated within a potential model using the same real central potential both in the entrance and exit channels. According to our calculations, different potential choices in these channels change  $\sigma_{n,\gamma}$  by only 1%. Absorption from the entrance channel is neglected because, according to our estimation within a coupled-channel model, they change  $\sigma_{n,\gamma}$  at the astrophysical energies by no more than 0.5%.

The numerical values of  $S(0)$ ,  $s_1$  and  $s_2$  are given in Table II, calculated with the parameters  $V_0$ ,  $r_0$ ,  $a$ , and  $S_{\text{mir}}$  from the same table. The main contribution to  $S(0)$  comes from large  $r$  and it is almost entirely determined by  $C_n^2$ . With fixed  $C_n^2$ , the residual uncertainty in  $S(0)$  due to different geometries of the potential well is only 1%. The other coefficients,  $s_1$  and  $s_2$ , are more sensitive to the potential choice: 3% and 10%, respectively. The resulting value of  $\sigma_{n,\gamma}(23.3 \text{ keV})$  is  $5.3 \pm 0.3 \mu\text{b}$ , which is consistent with the first theoretical potential model calculations from Ref. [5].

Figure 2 shows  $\sigma_{n,\gamma}E^{-1/2}$  derived from mirror symmetry by the dark shadowed area. The light shadowed area corresponds to calculations with all other  $E_R$  and  $\Gamma_p$  consistent with the condition  $S_{\text{mir}} \leq 1.15$ . Our  $\sigma_{n,\gamma}$  are smaller than the previous MCM results of Ref. [7]. This is explained by the overestimation of  $C_n^2$  in the MCM with the V2 forces, which is known for other nuclei. Our predictions agree with indirect determinations from Refs. [9,10] but they do not leave any room for small  $\sigma_{n,\gamma}$ . Reciprocally, small  $\sigma_{n,\gamma}$  from Refs. [4,8,11] would correspond to smaller  $C_n^2$  and, therefore, a smaller width of  $^{15}\text{F}(\frac{1}{2}^+)$ ,  $\Gamma_p \sim 280 \text{ keV}$  provided  $E_R = 1.47 \text{ MeV}$ . The narrower width would make the experimental determination of  $E_R$  and  $\Gamma_p$  much easier and would have not caused the currently existing spread in their values.

In summary, the charge symmetry of the  $^{15}\text{C} \rightarrow ^{14}\text{C} + n$  and  $^{15}\text{F} \rightarrow ^{14}\text{O} + p$  decays offers a strong test for the direct  $E1$   $^{14}\text{C}(n, \gamma)^{15}\text{C}$  cross sections. It significantly reduces the uncertainty in the current knowledge of the  $^{14}\text{C}(n, \gamma)^{15}\text{C}$  cross sections and favors the earlier theoretical predictions for this reaction from Ref. [5]. It also shows that directly and some indirectly measured cross sections in [4,8,11] strongly contradict charge symmetry in the  $^{15}\text{C}$ - $^{15}\text{F}$  mirror pair. This contradiction deserves thorough attention because it brings into question the determination of the astrophysically important  $(n, \gamma)$  cross sections for short-lived radioactive targets.

N.K.T. thanks T. Nakamura for communicating the  $\sigma_{n,\gamma}(23.3 \text{ keV})$  value and T. Aumann for useful discussions. She also gratefully acknowledges support from the UK EPSRC via Grant No. GR/T28577.

- [1] T. Kajino, G.J. Matthews, and G.M. Fuller, *Astrophys. J.* **364**, 7 (1990).
- [2] M. Wiescher, J. Görres, and H. Schatz, *J. Phys. G* **25**, R133 (1999).
- [3] T. Sasaqui *et al.*, *Astrophys. J.* **634**, 1173 (2005).
- [4] H. Beer *et al.*, *Astrophys. J.* **387**, 258 (1992).
- [5] M. Wiescher, J. Görres, and F.K. Thielemann, *Astrophys. J.* **363**, 340 (1990).
- [6] H. Herndl *et al.*, *Phys. Rev. C* **60**, 064614 (1999).
- [7] P. Descouvemont, *Nucl. Phys.* **A675**, 559 (2000).
- [8] Á. Horváth *et al.*, *Astrophys. J.* **570**, 926 (2002).
- [9] U. Datta Pramanik and (LAND-CB-FRS-Collaboration), *Prog. Theor. Phys. Suppl.* **146**, 427 (2002).
- [10] T. Nakamura *et al.*, *Nucl. Phys.* **A722**, C301 (2003); T. Nakamura (private communication).
- [11] R. Reifarh *et al.*, *Nucl. Phys.* **A758**, 787c (2005).
- [12] N.K. Timofeyuk, R.C. Johnson, and A.M. Mukhamedzhanov, *Phys. Rev. Lett.* **91**, 232501 (2003).
- [13] N.K. Timofeyuk and P. Descouvemont, *Phys. Rev. C* **72**, 064324 (2005).
- [14] D. Baye, P. Descouvemont, and F. Leo, *Phys. Rev. C* **72**, 024309 (2005).
- [15] A.B. Volkov, *Nucl. Phys.* **74**, 33 (1965).
- [16] D.R. Thompson, M. LeMere, and Y.C. Tang, *Nucl. Phys.* **A286**, 53 (1977).
- [17] D. Baye and N. Pecher, *Bull. Cl. Sci., Acad. R. Belg.* **67**, 835 (1981).
- [18] V.Z. Goldberg *et al.*, *Phys. Rev. C* **69**, 031302(R) (2004).
- [19] J.D. Goss *et al.*, *Phys. Rev. C* **12**, 1730 (1975).
- [20] P. Capel, D. Baye, and V.S. Melezhik, *Phys. Rev. C* **68**, 014612 (2003).
- [21] U.D. Pramanik *et al.*, *Phys. Lett.* **551B**, 63 (2003).
- [22] J.R. Terry *et al.*, *Phys. Rev. C* **69**, 054306 (2004).
- [23] W. Benenson *et al.*, *Phys. Rev. C* **17**, 1939 (1978).
- [24] G.J. KeKelis *et al.*, *Phys. Rev. C* **17**, 1929 (1978).
- [25] W.A. Peters *et al.*, *Phys. Rev. C* **68**, 034607 (2003).
- [26] A. Lepine-Szily *et al.*, *Nucl. Phys.* **A722**, C512 (2003).
- [27] F.Q. Guo *et al.*, *Phys. Rev. C* **72**, 034312 (2005).
- [28] D. Baye, *Phys. Rev. C* **70**, 015801 (2004).